Evaluation of atmospheric dilution factors for effluents diffused from an elevated continuous point source

By H. BULTYNCK, *Studie Centrum voor Kernenergie (S.C.K./C.E.N.), Mol,* and L. M. MALET, *Institut Royal Météorologique de Belgique (I.R.M.-K.M.I.), Uccle, Belgium*

ABSTRACT

Using the wind vector fluctuations measured at a height of 69 m by a tridimensional anemometer, the standard deviations σ_y and σ_z of the lateral and vertical distributions of the effluents emitted by an elevated continuous point source have been computed. Nearly 300 hourly tests covering most of the weather conditions to be encountered on the Mol site have been made, during which have also been determined the values of a stability parameter S defined as the ratio of the hourly mean of the vertical gradient of the potential temperature between 8 and 114 m to the square of the hourly mean wind speed at 69 m. The dependence functions $\sigma_{y \text{ or } z} = f(S)$ are of the hyperbolic type for $S > 0$ as well as for $S < 0$; they apply for hourly mean wind speeds up to 11.5 m s^{-1}. For the sake of simplicity and quick estimations of σ_y and σ_z for current practical uses, seven atmospheric stability categories have been defined with the corresponding median σ_y and σ_z values at different downwind distances x. When $\bar{u} < 11.5$ m.s^{-1}, categories E_1 to E_6 are differentiated by means of a parameter λ derived from S by $\lambda = \log_{10}[|S| \cdot 10^6]$; category E_7 corresponds to the case of strong winds. The data obtained show that for downwind distances x up to 50 km, the standard deviations σ_y and σ_z depend on x following a power law. The Mol theoretical results compare favourably with those found by means of field experiments carried out on the Mol site as well as elsewhere by other authors.

1. Position of the problem

From a public health point of view, the safe operation of nuclear research centres and power stations or conventional industrial plants can only be achieved if the diffusive properties of the first few hundred metres of the atmosphere over large areas around the sites are adequately known.

Such knowledge of the diffusive capacities of the lower atmosphere would allow us to (*a*) derive a working limit which may not be exceeded during routine releases of an effluent into the atmosphere, and to check whether the resulting concentrations due to these specified substances near the ground are within safe limits as regards the population in the neighbourhood; (*b*) take advantage of the most favourable meteorological conditions for special controlled releases of pollutant material the storage of which would otherwise entail considerable expense or other operational problems; and (*c*) to elaborate an effective environmental survey system and to provide an infrastructure for intervening in case of major pollution accidents.

For instance, it was desirable to calculate at any point around the S.C.K./C.E.N. nuclear site, the mean concentration over a given time interval, $\bar{\chi}$ (Ci m^{-3}), of the substances diffused in a turbulent atmosphere from a point source (reactor or laboratory stacks) with continuous release of intensity Q (Ci s^{-1}) situated at a height of about 60 m above the ground.

$\bar{\chi}$ is given by the fundamental relation

$$\bar{\chi} = Q\delta_a^{-1} \tag{1}$$

where δ_a(m^3 s^{-1}) is the atmospheric dilution factor depending on the diffusive capacities of the atmosphere resulting from the turbulence and the transport action of the wind.

Whatever the question may be, to compute concentrations due to short or long duration releases, it is essential to dispose of the dilution factors and consequently of the diffusive capacities of the atmosphere relating to the various possible meteorological conditions.

The atmospheric diffusion parameters may be obtained from a straight statistical treatment of series of observations of the fluctuating wind vector following an appropriate mathematical model. However, this direct method, which is the best possible, implies an important instrumental infrastructure, considerable means for electronic computation and the intervention of a highly qualified staff. Furthermore, this method is time-consuming, unsuitable for continuous monitoring and, then, not compatible with the setting up of an alarm system. Consequently, an indirect method has to be found which should at the same time be sufficiently reliable and easy to use in current practice by non-specialists.

Such a method consists in bringing into evidence some relationship which could exist between the diffusive capacities of the atmosphere and a parameter, easily and continuously measurable, characteristic of the state of stability of the air within the layer wherein the effluents diffuse.

Concrete results based on a long series of observations of the fluctuations of the wind vector on the site of S.C.K./C.E.N. have been obtained in that field. They have been published in a fully detailed S.C.K./C.E.N. report (1) and applied in another (2).

The purpose of the present paper is to give the essential features of these reports and to ensure them of a wider audience.

2. Direct evaluation of the diffusive capacities of the atmosphere within the boundary layer

2.1. Basic hypotheses

The turbulent diffusion model choosen is based on the following hypotheses:

2.1.1. The turbulence is homogeneous and stationary; in other words, all other things being equal, the diffusive properties of the atmosphere are supposed constant in the time and space intervals considered.

2.1.2. The release is continuous. This implies that the duration of the sampling may not exceed the duration of the release. For practical reasons, the concentrations $\bar{\chi}$ are averaged over one hour. Instantaneous concentrations may depart significantly from $\bar{\chi}$ values; they are not taken into account in the present paper.

2.1.3. The concentrations of substances in a horizontal and in a vertical plane within the plume are normally distributed. It is then possible to express the concentrations $\bar{\chi}$ at any point (xyz) as a function of the standard deviations $\sigma_y(x)$ and $\sigma_z(x)$ of the cross-wind and vertical distributions.

2.1.4. The mean wind direction does not vary with height. The fact that this hypothesis is not verified leads to errors by excess in the concentration values because the horizontal dispersion is underestimated.

2.1.5. The mean wind speed does not vary with height during the sampling time interval: $\bar{u}(z) = \text{constant}$.

2.2. Expression of the mean concentrations $\bar{\chi}$

Any turbulent flow may be described as the superimposition of eddies on the mean flow. Thus, the instantaneous velocity of the particles in the plume diffused by the turbulent atmosphere is given by:

$$U = \bar{U} + U' \tag{2}$$

where

U is the instantaneous wind vector at time t,

$\bar{U}$ is the hourly mean wind vector, and

U' is the fluctuation from the mean wind vector observed at time t; one has $\bar{U}' = 0$.

If the origin of an orthogonal coordinate system (right-handed) is placed at the origin of the mean wind vector in such a way that the x-axis coincides with this vector direction, the components of the instantaneous wind vector U assume the simplified form:

$$\begin{aligned} u &= \bar{u} + u' \\ v &= v' \\ w &= w' \end{aligned} \tag{3}$$

The above-mentioned hypotheses being accepted, the spatial distribution of the substances released may be expressed by:

$$\bar{\chi}(xyz) = \frac{Q}{2\pi\bar{u}\sigma_y(x)\,\sigma_z(x)} \exp\left[-\frac{y^2}{2\sigma_y^2(x)}\right] \times \exp\left[-\frac{z^2}{2\sigma_z^2(x)}\right] \tag{4}$$

where

$\bar{u}$ is the hourly mean wind speed (m s^{-1});

$\sigma_y(x)$ and $\sigma_z(x)$ (m) are the standard deviations of the cross-wind and vertical distributions. They characterize the diffusive capacity of the atmosphere within which the effluents are released and may be expressed respectively in terms of the turbulent components v' and w' of the wind.

Equation (4) shows that, following the diffusion model adopted, the concentration of materials at any point (xyz) is: (i) proportional to the source strength Q, (ii) inversely proportional to the dimension and form of the plume diffused expressed by the factors $\sqrt{2\pi}\,\sigma_y(x)$ and $\sqrt{2\pi}\,\sigma_z(x)$, i.e. to the diffusive capacity of the atmosphere, and (iii) inversely proportional to the transport action of the wind speed $\bar{u}$.

2.3. Standard deviations

It has been shown, namely in (1), that, at distance x from the source, the standard deviations $\sigma_y(x)$ and $\sigma_z(x)$ of the cross-wind and vertical distributions may be expressed as follows:

$$\sigma_y(x) = \left[\overline{\frac{\overline{v_x'^2}}{\beta_y \bar{u}}}\right]_B^{\frac{1}{2}} \frac{x}{\bar{u}} \tag{5}$$

$$\sigma_z(x) = \left[\overline{\frac{\overline{w_x'^2}}{\beta_z \bar{u}}}\right]_B^{\frac{1}{2}} \frac{x}{\bar{u}} \tag{6}$$

where

A) $\left[\overline{\frac{\overline{v_x'^2}}{\beta_y \bar{u}}}\right]_B$

and

$\left[\overline{\frac{\overline{w_x'^2}}{\beta_z \bar{u}}}\right]_B$

are the running means over an averaging time $T = x/\beta_y \bar{u}$ or $x/\beta_z \bar{u}$ during a sampling interval $B = 1$ hour;

B) β_y and β_z depend on the existing relation between the Lagrangian and the Eulerian time scales of turbulence; following Wandel & Kofoed-Hansen (3) β_y and β_z have been expressed by:

$$B_y = \frac{\sqrt{\pi}}{4}\,\bar{u}(\overline{v'^2})^{-\frac{1}{2}} \tag{7}$$

$$\beta_z = \frac{\sqrt{\pi}}{4}\,\bar{u}(\overline{w'^2})^{-\frac{1}{2}} \tag{8}$$

C) $\bar{u}$ is the hourly mean speed;
D) x is the down-wind distance.

3. Atmospheric stability parameter

3.1. Several parameters have already been proposed to characterize the atmospheric stability; among them:

3.1.1. The Monin-Obukhov (4) parameter z/L, where z is the height (m) and L the Monin length given by:

$$L = -\frac{u_*^3 c_p \varrho \theta^\circ}{kgQ_H} \text{ (m)}$$

where

u_* is the friction velocity (m s^{-1}),
c_p is the specific heat of the air at constant pressure (cal g^{-1} °K^{-1})
ϱ is the mass density of the air (g m^{-3}),
θ° is the absolute temperature (°K)
k is the Karman's constant
Q_H is the vertical heat flux (cal m^{-2} s^{-1}), and
g is the acceleration due to gravity (m s^{-2})

3.1.2. The Richardson number

$$\mathrm{Ri} = \frac{g}{\bar{\theta}^\circ} \frac{\frac{\partial\theta}{\partial z}}{\left(\frac{\partial\bar{u}}{\partial z}\right)^2}$$

where

$\frac{\partial\theta}{\partial z}$ is the vertical gradient of the potential temperature
$\frac{\partial\bar{u}}{\partial z}$ is the vertical shear of the mean wind speed
$\bar{\theta}^\circ$ is the mean absolute temperature (°K), and
g is the acceleration due to gravity.

3.1.3. It will be noted that the determination of L requires measurements of quantities (namely u_* and Q_H) not easy to obtain in current practice and that the vertical shear which appears as a square in the denominator of Ri is also difficult to measure with the required accuracy.

3.2. To avoid these difficulties, the following parameter has been adopted after a number of comparative tests:

$$S=\frac{\frac{\partial\theta}{\partial z}}{\bar{u}^2_{69\mathrm{m}}} \tag{9}$$

where $\frac{\partial\theta}{\partial z}$ is the vertical gradient of the mean potential temperature in the layer 8 to 114 m

and $\bar{u}_{69\mathrm{m}}$ is the mean wind speed at the height of 69 m.

Studies of the wind profiles between 2 and 120 m have shown that the parameter S is univocally bound to the Monin-Obukhov length L.

The wind speed at other heights differs from the wind speed at 69 m by an amount which grows as the vertical temperature gradient becomes more positive; however, experience has shown that the height (between 24 and 120 m) at which the wind speed is measured does not matter very much as far as the quality of the correlation between S and σ_y or σ_z is concerned.

The height of 69 m has been explicitly chosen because it is the height of the S.C.K./C.E.N. reactor stacks and especially because the wind speed and the fluctuations of the wind vector could be measured simultaneously by the same instrument, namely a vectorial anemograph Kirem (see (1) chap. I).

U. Högström (5) has also worked with a similar S parameter but with $\bar{u}$ measured at a height of 500 m, $\bar{u}_{500\,\mathrm{m}}$ being assumed representative of the mean flow of the air above the friction layer. Tests in that field were made using the data given in the aerological soundings of the station UCCLE-Brussels (at about 80 km south of Mol); they were not satisfactory. One must admit that the radar or radiotheodolite winds in the first few hundred metres are often erroneous due to the great difficulties encountered in aiming accurately at the moving target at the beginning of an ascent.

4. Observations, computation of σ_y, σ_z and S

4.1. From January 1966 to July 1968, 280 hourly observations were performed in order to cover satisfactorily the atmospheric conditions encountered in the Mol area and, consequently, to compute as well as possible the correlation between σ_y or σ_z on one hand and S on the other.

For each period of observation (see (1) chapters I and II), the following data were recorded on punched cards and on point recorders: (*a*) values of the intensity ϱ(m/s^{-1}), direction from the North θ(°) and inclination from the horizontal plane ϕ(°) of the wind vector at a height of 69 m; all these data being measured by a vectorial anemometer at the rate of one set of data every 9 seconds; (*b*) values of the temperature measured every 36 seconds by thermocouples Cu-Constantan installed at 2, 8, 24, 49, 78 and 114 m; (*c*) values of the horizontal wind speed measured every 9 seconds by Lambrecht anemometers installed at 24, 49,78 and 114 m.

These data have in the first place been used to check how far the basic hypotheses concerning behaviour of the atmosphere during each test had been verified.

4.1.1. *Covariances*

The covariances $\overline{(u'v'_T)_B}$, $\overline{(u'w'_T)_B}$ and $\overline{(v'w'_T)_B}$ have been computed using a growing averaging time T. It is well known that $\overline{(u'v'_T)_B}$ and $\overline{(v'w'_T)_B}$ must be very near zero or, at least, tend rapidly towards 0 when T increases. Furthermore, $\overline{(u'w'_T)_B}$ is negative and its absolute value must be much greater than that of the two other covariances. When these rules were not observed during the course of a test, the latter has been discarded.

4.1.2. *Normality of distributions of angular data*

To check the normality of the distributions of the angular data θ and ϕ the form factors FF(6) have been used:

$$FF_L=\frac{\sqrt{\overline{\theta^2}}}{\overline{|\theta|}}$$

and

$$FF_V=\frac{\sqrt{\overline{\phi^2}}}{\overline{|\phi|}}$$

where θ and ϕ are the angular deviations respectively from the North and the horizontal.

If the θ's and ϕ's are normally distributed, the factors FF are equal to $\sqrt{\pi/2}$; a tolerance of 10 % is however admissible. As a matter of fact, 97 % of the θ and 87 % of the ϕ distributions could be accepted as normal in the whole series of the S.C.K./C.E.N. tests.

4.1.3. *Variations of vertical profiles of wind speed and temperature*

The Richardson number Ri is expressed as a function of the vertical wind shear and the potential temperature gradient along the ascending vertical; it is therefore convenient to appreciate the variations of these parameters in sub-layers. For each test, the successive 10-minute-means of the temperature and the wind speed measured at different levels along the meteorological tower (6 for the temperature and 4 for the wind speed) were computed. With these computed data, it was possible to determine a global Richardson number (7).

To do this, the intermediate Richardson numbers for levels i and j had first to be calculated using:

$$(\mathrm{Ri})_{i,j} = \frac{2gz_{ij} \ln n_{ij}(\theta_j - \theta_i)}{\theta^{\circ}(u_j - u_i)}$$

where

$$z_{ij} = \sqrt{z_i z_j}$$

and

$$n_{ij} = \sqrt{z_j/z_i}$$

z_i and z_j being the heights of the levels i and j respectively. Five values of z_{ij} were retained: $z_{13} = 6.9$ m; $z_{15} = 12.5$ m; $z_{34} = 34.3$ m; $z_{45} = 61.8$ m; $z_{56} = 94.3$ m.

The global Richardson number (Ri)′ was then obtained by computing:

$$(\mathrm{Ri})' = \frac{\sum (\mathrm{Ri})_{ij}}{\sum z_{ij}}$$

which may be accepted as an approximation of the vertical gradient of Ri

$$(\mathrm{Ri})' \simeq \frac{\partial(\mathrm{Ri})}{\partial z}$$

Only those tests were kept for further study during the course of which (Ri)′ remained reasonably constant.

4.2. Computation of standard deviations σ_y and σ_z and of corresponding S values

For each acceptable test, S was computed applying relation (9) whilst relations (5) and (6) were used to obtain $\sigma_y(x)$ and $\sigma_z(x)$ at different downwind distances, x equal to $T\beta_y \bar{u}$ and $T\beta_z \bar{u}$ respectively, T being the averaging time interval.

With these data at hand, it was very easy to determine the σ_y and σ_z values at a certain number of fixed distances from the source: 100, 500, 1 000, 5 000, 10 000 m. The method mostly used for this was graphical interpolation. For a few cases only ($x = 100$ m, $S > 0$) extrapolation was required.

5. Dependence of the standard deviations σ_y and σ_z on atmospheric stability

In order to put into evidence a law of dependence of the standard deviations σ_y and σ_z of the cross-wind and vertical distributions of materials suspended in the plume on the state of stability of the air in the friction layer characterized by S, it has been thought useful to proceed as follows. The tests compatible with the basic hypotheses of the diffusion model have been separated into two parts following the sign of S. Each part has then been divided into groups including, as far as possible, the same number of tests and each group has been characterized by the group-means of σ_y or σ_z on the one hand and of S on the other. As explained hereafter, tests where $u69\,\mathrm{m} > 11.5$ m s^{-1} have been set apart for special analysis; they are thus not taken into account in the groups mentioned above.

Tables 1 to 4 show the results of this grouping.

5.1. Analytical form of dependence

Whatever the value of x(100, 500, 1 000, 5 000, 10 000 m), if the points (S, σ_y) or (S, σ_z) are noted on a rectangular diagram with σ_y or σ_z as ordinate and S as abscissa and if a line is drawn to adjust these points, one gets a curve shaped as an elongated letter S stretched at both its superior and inferior ends. The curve is asymmetric and articulated on the value

Table 1. $\sigma_y(x, |S|)$ for $S > 0$

$x = 100$ m				$x = 500$ m				$x = 1\,000$ m				$x = 5\,000$ m				$x = 10\,000$ m			
N	$\bar{S}$	$\bar{\sigma}_y$	$\bar{\sigma}_{y\,calc}$	N	$\bar{S}$	$\bar{\sigma}_y$	$\bar{\sigma}_{y\,calc}$	N	$\bar{S}$	$\bar{\sigma}_y$	$\bar{\sigma}_{y\,calc}$	N	$\bar{S}$	$\bar{\sigma}_y$	$\bar{\sigma}_{y\,calc}$	N	$\bar{S}$	$\bar{\sigma}_y$	$\bar{\sigma}_{y\,calc}$
2	5 520	7	9.2	2	5 520	31.5	33.5	2	5 520	58.5	57.3	2	5 520	255	201	1	6 600	500	358
7	643	10.9	9.7	7	643	34.1	35.4	7	643	56.6	60.5	7	643	186	212	5	607	364	380
10	212	12.7	10.6	11	192	41.9	39.2	11	192	70.8	67.0	10	197	228	234	7	206	408	416
7	84.5	14.2	12.0	7	84.5	48.1	43.8	9	82.6	75.8	74.8	7	84.5	262	262	4	89	516	464
8	50.1	16.9	12.8	8	50.1	49.8	46.9	8	50.1	80.0	80.2	7	48	257	283	5	47	442	507
6	27.0	18.7	13.9	6	27.0	53.2	50.7	8	26.2	82.3	86.7	6	27	243	303	4	26	362	543
6	8.0	16.5	15.2	7	7.6	57.4	55.6	7	7.6	98.7	95.1	7	7.6	350	333	7	8	606	594

N = number of cases considered; S = mean atmospheric stability parameter ($10^{-6}.°C.s^2.m^{-3}$)
$\bar{\sigma}$ = mean standard deviation (m); $\bar{\sigma}_{calc}$ = mean standard deviation computed from eq. 11 or 12 (m).

Table 2. $\sigma_y(x, |S|)$ for $S < 0$

$x = 100$ m				$x = 500$ m				$x = 1\,000$ m				$x = 5\,000$ m				$x = 10\,000$ m			
N	$\bar{S}$	$\bar{\sigma}_y$	$\bar{\sigma}_{y\,calc}$	N	$\bar{S}$	$\bar{\sigma}_y$	$\bar{\sigma}_{y\,calc}$	N	$\bar{S}$	$\bar{\sigma}_y$	$\bar{\sigma}_{y\,calc}$	N	$\bar{S}$	$\bar{\sigma}_y$	$\bar{\sigma}_{y\,calc}$	N	$\bar{S}$	$\bar{\sigma}_y$	$\bar{\sigma}_{y\,calc}$
9	20	18.6	16.9	9	20.3	61.9	61.9	10	19.0	106.2	105.4	10	19.0	375	369	10	19.0	643	659
9	48	19.3	18.1	10	47.3	66.1	66.0	10	47.3	113.3	112.8	10	47.3	390	395	9	47.6	644	706
10	70.8	19.9	18.9	10	70.8	68.8	69.2	10	70.8	118.1	118.4	10	70.8	408	414	8	69.1	733	738
9	105	21.1	20.1	9	105	73.2	73.6	9	105	125.9	125.7	9	105	422	440	6	106	705	786
10	137	19.8	21.1	10	137	73.0	77.2	10	137	128.2	131.9	9	139	451	463	5	137	788	824
10	247	22.2	23.9	10	247	84.3	87.3	10	247	147.1	149.2	10	247	521	522	7	224	867	912
10	450	24.5	27.3	10	450	98.9	99.8	10	450	173.9	170.6	7	454	629	599	4	462	1 038	1 069
10	607	28.8	29.1	10	607	106.5	106.4	10	607	183.9	181.9	6	598	622	635	1	1 100	1 500	1 269
10	1 094	30.7	32.4	10	1 094	117.3	118.6	10	1 094	202.5	202.7	2	1 100	790	711				
3	1 630	35.0	34.4	3	1 630	128.7	125.6	3	1 630	213.3	214.7								

For explanation of symbols, see Table 1.

Table 3. $\sigma_z(x, |S|)$ for $S > 0$

$x = 100$ m				$x = 500$ m				$x = 1\,000$ m				$x = 5\,000$ m				$x = 10\,000$ m			
N	$\bar{S}$	$\bar{\sigma}_z$	$\bar{\sigma}_{z\,\text{calc}}$	N	$\bar{S}$	$\bar{\sigma}_z$	$\bar{\sigma}_{z\,\text{calc}}$	N	$\bar{S}$	$\bar{\sigma}_z$	$\bar{\sigma}_{z\,\text{calc}}$	N	$\bar{S}$	$\bar{\sigma}_z$	$\bar{\sigma}_{z\,\text{calc}}$	N	$\bar{S}$	$\bar{\sigma}_z$	$\bar{\sigma}_{z\,\text{calc}}$
7	12 840	6.1	7.4	7	12 840	24.0	23.4	7	12 840	41.7	38.4	7	12 840	152	118	5	9 450	300	195
10	716	8.4	8.5	10	716	25.5	27.0	10	716	41.6	44.3	10	716	134	137	7	730	236	224
9	313	10.6	9.6	10	316	29.9	30.3	10	316	45.9	49.6	8	329	123	152	6	343	203	248
7	162	11.6	10.6	8	166	33.9	33.6	10	169	52.8	54.9	8	163	163	170	4	165	252	279
8	89	13.7	11.6	10	89	41.3	36.9	10	89	65.9	60.4	10	89	198	186	8	89	315	306
5	51	13.8	12.4	7	55	42.1	39.0	10	57	63.9	63.7	5	55	208	197	2	50	420	327
5	30	19.0	13.0	6	30	49.3	41.1	10	31.5	69.2	67.2	7	29	190	208	3	32	323	340
10	11.1	13.9	13.6	12	10.5	45.8	43.2	14	11.5	72.7	70.6	12	11.1	230	218	11	11	381	358

For explanation of symbols, see Table 1.

Table 4. $\sigma_z(x, |S|)$ for $S < 0$

$x = 100$ m				$x = 500$ m				$x = 1\,000$ m				$x = 5\,000$ m				$x = 10\,000$ m			
N	$\bar{S}$	$\bar{\sigma}_z$	$\bar{\sigma}_{z\,\text{calc}}$	N	$\bar{S}$	$\bar{\sigma}_z$	$\bar{\sigma}_{z\,\text{calc}}$	N	$\bar{S}$	$\bar{\sigma}_z$	$\bar{\sigma}_{z\,\text{calc}}$	N	$\bar{S}$	$\bar{\sigma}_z$	$\bar{\sigma}_{z\,\text{calc}}$	N	$\bar{S}$	$\bar{\sigma}_z$	$\bar{\sigma}_{z\,\text{calc}}$
4	20	15.3	14.3	6	19	47.0	45.4	10	18.2	73.4	74.4	8	21	220	230	5	22	362	377
8	34	15.8	14.7	10	39	46.9	46.4	10	39	72.4	76.0	9	39	210	234	7	38	349	385
7	60	15.1	14.9	9	60	46.9	47.2	10	60	76.0	77.6	8	61	238	239	5	59	418	392
5	72	17.4	15.0	8	73	48.6	47.9	10	72	74.5	78.4	7	73	224	242	3	70	333	396
9	94	15.8	15.5	9	94	49.1	49.0	10	94	78.3	80.0	8	92	241	245	5	94	412	407
9	114	17.3	15.8	9	114	48.6	49.9	10	113	77.5	81.4	7	113	205	250	3	112	360	410
8	152	16.4	16.2	10	149	51.3	51.3	10	149	82.9	83.9	7	155	247	259	3	167	450	432
10	251	16.9	17.5	10	251	56.4	55.2	10	251	94.1	90.7	9	244	292	279	4	245	537	459
10	444	17.8	19.7	10	444	59.4	62.4	10	444	97.9	102.2	6	437	282	313	2	453	640	521
10	567	19.7	21.0	10	567	69.2	66.3	10	567	117.2	108.8	7	552	350	333	4	915	402	633
10	979	22.8	24.6	10	979	76.0	78.0	10	979	125.0	127.5	4	914	343	385				
(4)	(1 587)	(27.0)		(4)	(1 587)	(91.5)		(4)	(1 587)	(153.2									

For explanation of symbols, see Table 1.

$\sigma_y(x, 0)$ or $\sigma_z(x, 0)$ towards which σ_y or σ_z tends when $\left|\frac{\partial\theta}{\partial z}\right|$ and consequently $|S|$ vanish.

To obtain a satisfactory analytical expression of the dependence relation

$$\sigma_{y\,\mathrm{or}\,z}(x, S) = f(S)$$

the parts of the curve situated respectively on the negative (unstability) and the positive (stability) sides of S have been considered separately.

It has been found (1 chap. V, § 1 to 3) that each of these curve segments could reasonably be assimilated to a segment of an equilateral hyperbola limited at one end by the value $\sigma_{y\,\mathrm{or}\,z}(x, 0)$.

Thus for any downwind distance x, the dependence relation may be written as:

$$\sigma_{y\text{ or }z}(z, |S|) = \sigma_{y\text{ or }z}(x, 0)\left[\frac{b + c\,|S\,10^6|}{b + |S\,10^6|}\right] \tag{10}$$

where b and c are constants.

This type of relation, restricted to σ_z and a stable atmosphere, has already been proposed by U. Högström (5). The individual $\sigma_{y\,\mathrm{or}\,z}$ data for the downwind distance $x = 1\,000$ m are the most numerous and none of them results from extrapolation; they may then be considered as the most accurate of the whole lot grouped in Tables 1 to 4. That is the reason why they have exclusively been used to determine the values of b and c in (10) by the least squares method applied to a system of m non-linear equations with n unknowns (8).

This mathematical process has led to the following results:

for $S > 0: \sigma_y(x, |S|)$

$$= \sigma_y(x, 0)\left[\frac{60 + 0.57\,|S10^6|}{60 + |S10^6|}\right] \tag{11,1}$$

for $S < 0: \sigma_y(x, |S|)$

$$= \sigma_y(x, 0)\left[\frac{510 + 2.5\,|S10^6|}{510 + |S10^6|}\right] \tag{11,2}$$

for $S > 0: \sigma_z(x, S)$

$$= \sigma_z(x, 0)\left[\frac{158 + 0.52\,|S10^6|}{158 + |S10^6|}\right] \tag{12,1}$$

for $S < 0: \sigma_z(x, S)$

$$= \sigma_z(x, 0)\left[\frac{2\,480 + 3.63\,|S10^6|}{2\,480 + |S10^6|}\right] \tag{12,2}$$

Applied to the different sets of data given in Tables 1 to 4, the hereabove mentioned mathematical process has also led to:

$\sigma_y(100 \text{ m}, 0) = 16$ m and

$\sigma_z(100 \text{ m}, 0) = 14.1$ m

$\sigma_y(500 \text{ m}, 0) = 58.5$ m and

$\sigma_z(500 \text{ m}, 0) = 44.5$ m

$\sigma_y(1\,000 \text{ m}, 0) = 100$ m and

$\sigma_z(1\,000 \text{ m}, 0) = 73$ m

$\sigma_y(5\,000 \text{ m}, 0) = 350$ m and

$\sigma_z(5\,000 \text{ m}, 0) = 225$ m

$\sigma_y(10\,000 \text{ m}, 0) = 625$ m and

$\sigma_z(10\,000 \text{ m}, 0) = 370$ m

It must be noticed that the horizontal asymptote of each segment of equilateral hyperbola, the equation of which writes:

$$\sigma_{y\,\mathrm{or}\,z}(x, |S|) = c\sigma_{y\,\mathrm{or}\,z}(x, 0)$$

represents the limit towards which the standard deviation $\sigma_{y\,\mathrm{or}\,z}$ tends when $|S|$ grows. The vertical asymptote is situated further than the limiting value $\sigma_{y\,\mathrm{or}\,z}(x, 0)$ and must therefore not be taken into account.

Finally, it must be kept in mind that relations (11.1 and 11.2) and (12.1 and 12.2) apply when the hourly mean speed $\bar{u}$ is less than 11.5 m s^{-1}.

5.2. Graphical representation of dependence

In order to make easier the graphical representation of the dependence of $\sigma_{y\,\mathrm{or}\,z}$ on the state of stability of the air within the friction layer, a parameter λ derived from S by the formula

$$\lambda = \log_{10}[|S| \times 10^6] \tag{13}$$

has been adopted.

The curves of the Figs. 1 and 2 give the variations of σ_y and σ_z as a function of λ for $S > 0$ and $S < 0$ and for $x = 100$, 1 000, 10 000 m.

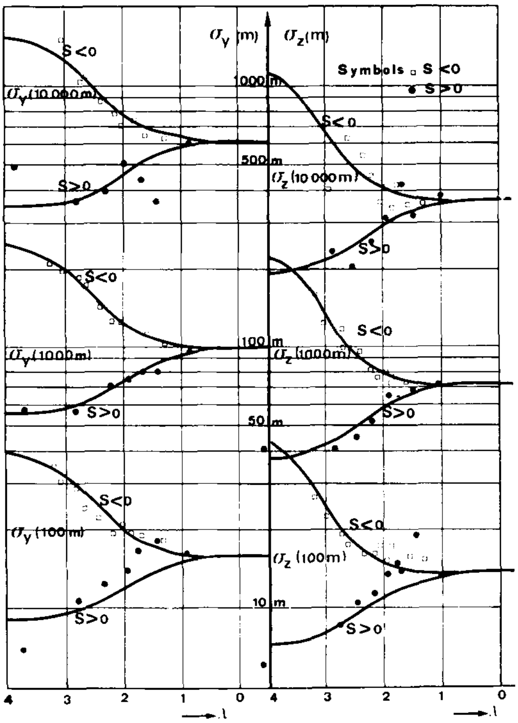

Fig. 1–2

For λ tending towards $-\infty$ (neutrality) one obviously has

$$\sigma_{y\,\mathrm{or}\,z}(x, |S|) = \sigma_{y\,\mathrm{or}\,z}(x, 0)$$

When S grows indefinitely, i.e. for great positive values of λ, one has

$$\sigma_{y\,\mathrm{or}\,z}(x, |S|) = c\sigma_{y\,\mathrm{or}\,z}(x, 0)$$

The small circles and crosses near the curves of Figs. 1 and 2 represent the actual values of $\sigma_{y\,\mathrm{or}\,z}$ found by grouping the tests data as mentioned before. It can be seen that their fitting to the computed curves is generally good. The largest discordances appear for $x = 100$ m both for σ_y and σ_z when $S > 0$. This is due to the fact that for this downwind distance most of the experimental σ data had to be extrapolated which implies that they have only an indicative value.

6. Quick estimation of σ_y and σ_z for practical uses

For the sake of simplicity and quick estimations of σ_y and σ_z for current practical uses, seven atmospheric stability categories have been defined with the corresponding σ_y and σ_z values at different downwind distances x. These categories are differentiated by means of the parameter λ following the way shown in Table 5.

Tables 6 and 7 show respectively the median values of the standard deviations σ_y and σ_z corresponding to each atmospheric equilibrium category at different downwind distances from the source.

6.1. Strong winds

It has been indicated above that the relations (11) and (12) only apply when $\bar{u} < 11.5$ m s^{-1}. In the case of strong winds, the state of stability of the atmospheric friction layer is always very near neutrality ($|S| \simeq 0$); but when $\bar{u}$ exceeds 11.5 m s^{-1}, the actual values of σ_y or σ_z at any distance x from the source are significantly greater than those arising from the computed curves shown in Figs. 1 and 2. This is especially true for short downwind distances.

It appears that the action of strong winds on obstacles disseminated on the ground around the source generates small eddies (mechanical turbulence due to surface roughness) which produce a greater diffusion. The effect diminishes with increasing distances. That is the reason why a special category E_7 has been defined based on the sole criterion: $u \geq 11.5$ m s^{-1}, in order to take these cases into particular account.

6.2. Frequencies of occurrence of stability categories

The frequencies of occurrence of the λ values have been computed for the S.C.K./C.E.N. site at Mol using continuous wind and temperature observations along the meteorological mast during the course of 1966 and 1967. The results are given in Table 8.

This table shows that during the two years considered, equivalent to 15 458 hours of observation:

S was greater than 0 in 70.9 % of the cases,
S was less than 0 in 24.2 % of the cases, and
$\bar{u}$ was greater than 11.5 m s^{-1} in 4.9 % of the cases.

Cases with $2 \leq \lambda \leq 3$ as well as for $S > 0$ than for $S < 0$ predominate; they correspond to mod-

Table 5

Atmospheric stability category	Differentiation criteria		
	$S > 0$	$S < 0$	
E_1	$\lambda \geqslant 2.75$		
E_2	$2.75 > \lambda > 1.75$		
E_3	$1.75 \geqslant \lambda$	$\lambda \leqslant 2$	$\bar{u} < 11.5$ m.s^{-1}
E_4		$2 < \lambda < 2.75$	
E_5		$2.75 < \lambda < 3.3$	
E_6		$3.3 \leqslant \lambda$	
E_7	$\bar{u} \geqslant 11.5$ m.s^{-1}		

Table 6. *Median values of* $\sigma_y = f(x, E_i)$ *(m)*

Atmospheric stability category	$x = 100$ m	$x = 500$ m	$x = 1\,000$ m	$x = 5\,000$ m	$x = 10\,000$ m
E_1	9.3	34	60	210	370
E_2	11	41	70	250	440
E_3	16	59	100	350	625
E_4	24	86	150	520	900
E_5	32	115	200	700	1 250
E_6	37	140	230	830	1 450
E_7	27	78	125	390	680

Table 7. *Median values of* $\sigma_z = f(x, E_i)$ *(m)*

Atmospheric stability category	$x = 100$ m	$x = 500$ m	$x = 1\,000$ m	$x = 5\,000$ m	$x = 10\,000$ m
E_1	8	25	43	130	210
E_2	10	33	55	170	270
E_3	14	45	73	225	370
E_4	18	58	94	280	460
E_5	25	82	135	400	660
E_6	35	110	180	560	920
E_7	17	55	86	240	380

erate winds (4 m s$^{-1} < \bar{u} < 7$ m s^{-1}). In fact, relations (11) and (12) have been established using tests with $\lambda < 4$ for $S > 0$ and $\lambda < 3.5$ for $S < 0$.

Table 8 shows that these intervals of λ values cover most of the meteorological situations encountered at Mol. Table 9 gives for the same period the frequencies of occurrence of the different stability categories defined above.

Conditions E_2 are the most frequent. They result either from an almost neutral thermal equilibrium with a moderate wind or from a slightly stable thermal equilibrium with a rather strong wind; both types of conditions are common in the Mol area. The wind mentioned hereabove refers to the height of 69 m.

6.3. Analytical representation of the dependence of $\sigma_{y\ \mathrm{or}\ z}$ on x for each stability category

Data from Tables 6 and 7 regarding the categories of atmospheric stability E_1 to E_7

Table 8

$\lambda = \log_{10}(\lvert S \rvert \times 10^6)$	%	%
$4.5 \leqslant \lambda < 5.0$	0.6	—
$4.0 \leqslant \lambda < 4.5$	1.4	0.1
$3.5 \leqslant \lambda < 4.0$	4.0	0.5
$3.0 \leqslant \lambda < 3.5$	9.2	2.5
$2.5 \leqslant \lambda < 3.0$	18.8	5.8
$2.0 \leqslant \lambda < 2.5$	18.5	6.7
$1.5 \leqslant \lambda < 2.0$	12.7	5.1
$1.0 \leqslant \lambda < 1.5$	4.5	2.9
$\lambda < 1.0$	1.2	0.7
	$S > 0$	$S < 0$

Table 9

Stability category	Frequency of occurrence (%)
E_1	24.7
E_2	34.3
E_3	20.5
E_4	9.6
E_5	4.2
E_6	1.8
E_7	4.9

show that, with a good approximation, the standard deviations may be written as follows:

$$\sigma_y(x) = Ax^a \tag{14}$$

$$\sigma_z(x) = Bx^b \tag{15}$$

for the downwind distance x comprised between 100 and 10 000 m and even extended to 50 000 m.

Such an analytical form has also been found by Healy (9) for $\sigma_y(x)$. The values of A, a, B and b are given in Table 10.

The use of the relations above leads to results differing by less than 5 % from the data of Tables 6 and 7; it greatly simplifies practical computations.

Table 10

Stability category	A	a	B	b
E_1	0.235	0.796	0.311	0.711
E_2	0.297	0.796	0.382	0.711
E_3	0.418	0.796	0.520	0.711
E_4	0.586	0.796	0.700	0.711
E_5	0.826	0.796	0.950	0.711
E_6	0.946	0.796	1.321	0.711
E_7	1.043	0.698	0.819	0.669

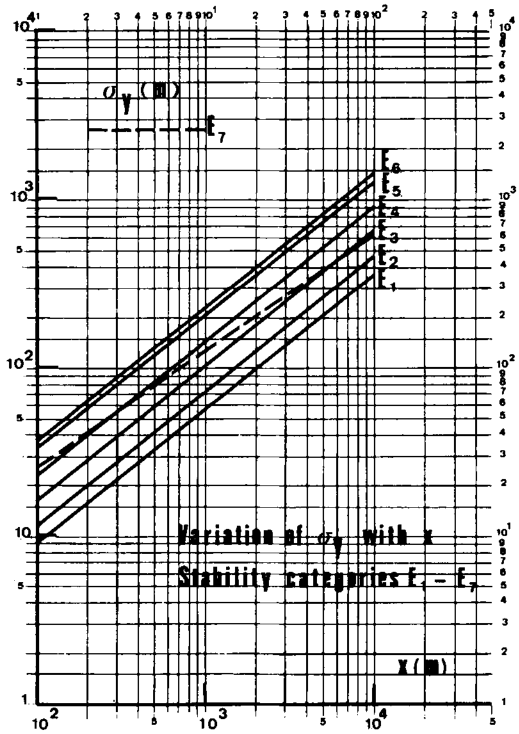

Fig. 3

Relations (14) and (15) are illustrated by Figs. 3 and 4. On these logarithmic diagrams, relations (14) and (15) take the form of parallel straight lines for categories E_1 to E_6.

The straight dotted line corresponding to E_7 shows that, at great downwind distances, E_7 behaves more or less like E_3 but that these two categories are quite different at short distances.

7. Comparison with other results

In order to appreciate how much confidence can be attributed to the results proposed in the present paper, it has been thought helpful to compare them with some other results obtained either by other authors or by another method.

7.1. Comparison with F. Pasquill's results

The values of the standard deviations of the cross-wind and vertical distributions of mat-

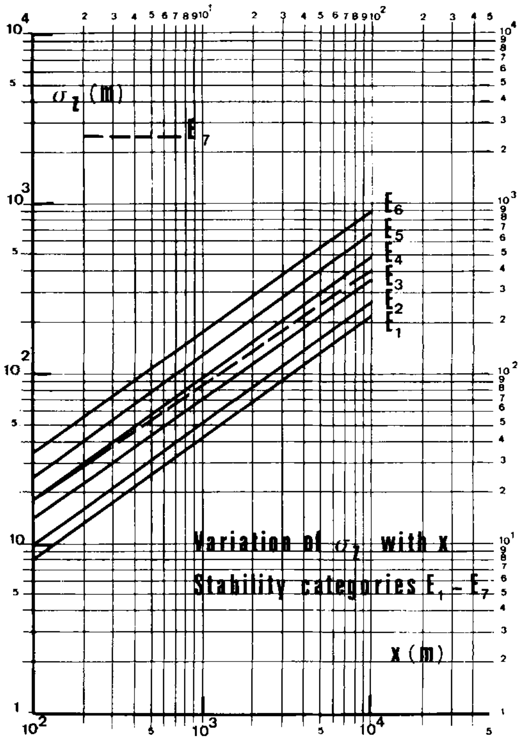

Fig. 4

ters in the plume worked out by F. Pasquill, (6) and (10), and presented by Hilsmeier-Gifford (11) in terms of σ_y and σ_z are at present moment employed by most users. These values are somewhat different from those proposed here.

7.1.1. At any given downwind distance, the range of variation of Pasquill's σ_y or σ_z's with the weather conditions is larger than that found on the Mol site. This fact is illustrated below; for example, at $x = 100$ m, one finds that:

Pasquill's σ_y's vary in the proportion of 1 to 6.3,

Mol σ_y's vary in the proportion of 1 to 4.1,

Pasquill's σ_z's vary in the proportion of 1 to 7.4,

Mol σ_z's vary in the proportion of 1 to 4.4.

7.1.2. At any given downwind distance, in neutral conditions. Pasquill's σ_y or σ_z is smaller than that found on the Mol site.

For example, at $x = 1\ 000$ m, one has:

σ_y(Pasquill) = 71 m and σ_y(Mol) = 100 m

σ_z(Pasquill) = 32 m and σ_z(Mol) = 73 m.

When the Mol σ_y and σ_z's are used for computation of the downwind distance $x_{\max}$ where the maximum ground concentration $\bar{\chi}_{\max}$ is to be found in different conditions of weather and effective height of the source, much smaller values are found than when applying Pasquill's data; the differences increase with the source height.

7.1.3. The causes of these differences are namely the following:

(*a*) Pasquill's σ_y and σ_z's were determined from the observation of angular fluctuations on anemometer traces; those proposed here have been obtained from the observation of the fluctuating wind vector. Therefore, the variations of the intensity ϱ of the wind vector are duly taken into account which is not the case for F. Pasquill.

(*b*) Pasquill's σ_y and σ_z's are given for sampling intervals not greater than 10 minutes, while the present work aims at determining hourly mean concentrations. When the atmosphere is very stable ($\lambda > 4$, $S > 0$) it is exceptional not to observe variations, often great variations, of the wind direction during an interval of 1 hour. The atmospheric stability category E_1 does not involve the conditions $\lambda \geqslant 4$ corresponding to the most stable Pasquill's weather type F. These conditions are not frequent on the Mol site for an elevated source (2 % during the course of 1966 and 1967) and, in such cases, application of the diffusion model appears questionable.

(*c*) Pasquill's σ_y and σ_z's have been determined for a source very near to or on the ground while herein they are given for a height of 69 m. It follows that the Mol σ_z's are greater than the Pasquill's ones, implying that the ground concentrations reach their maximum values nearer the source. In fact, the present work deals with an elevated source 69 m high. The results should not be applied without care to sources much higher or much below 69 m.

7.2. Comparison with Brookhaven National Laboratory (BNL–USA) and BEPO (Harwell–U.K.) results (12), (13), (14)

These results have been obtained in conditions of site, height of release and duration of observations very similar to those at Mol.

Table 11

Atmospheric stability category	σ_θ	C.E.N. σ_y (100 m)	C.E.N. σ_y (1 000 m)	B.N.L. σ_y (100 m)	B.N.L. σ_y (1 000 m)
E_1	5.6	8	60	9.5	56
E_2	6.3	10.5	70	10.7	63
E_3	9.2	16	100	16	92
E_4	14	24	150	24	140
E_5	18	32	200	31	180
E_6	21	37	250	36	210

(*a*) The BEPO's σ_z's are in good agreement with the Mol ones while the slope of the straight line representing $\log \sigma_y = f(x)$ is much greater for Mol than for BEPO (see figure 70 and 71 of (1), tome II).

(*b*) The BNL's σ_y's compare favourably with the Mol ones as shown in Table 11 which has been established using the reports $\sigma_y/\sigma_\theta = 1.7$ for $x = 100$ m and $\sigma_y/\sigma_\theta = 10$ for $x = 1\,000$ m (after (15) fig. 4.21).

7.3. Wind profiles

The study of wind profiles in neutral conditions may be used to check the computed σ_z's. In such conditions, the wind profile law writes:

$$\ln \frac{z + z_0 + d}{z_0} = k \frac{\bar{u}}{\bar{u}_*}$$

where

- z is the height above the ground (m),
- z_0 is the rugosity length (m),
- d is the zero plane displacement (m); so, d allows for the height of the obstacles on the site,
- $\bar{u}_*$ is the mean friction wind velocity (m s^{-1}),
- $\bar{u}$ is the mean speed at height z (m s^{-1}).

Using eight tests made in neutral conditions, it was found:

$$k \frac{\bar{u}}{\bar{u}_*} = 4.17 \quad \text{and } d = -10\,\text{m}$$

which leads to $z_0 = 0.92$ m.

One has:

$$\frac{\ln\left(\dfrac{z_1 + z_0 + d}{z_0}\right)}{\ln\left(\dfrac{z_2 + z_0 + d}{z_0}\right)} = \frac{\bar{u}_1}{\bar{u}_2}$$

The anemometers (Lambrecht type) installed at $z_1 = 24$ m and $z_2 = 49$ m gave $\bar{u}_1 = 5.6$ m s^{-1} and $\bar{u}_2 = 7.4$ m s^{-1}, means established on the whole duration of the eight considered neutral tests. So $\bar{u}_1/\bar{u}_2 = 0.757$ whilst the computation of the first member of the relation hereabove led to 0.756. The agreement is remarkable. Following the theory of G. I. Taylor as exposed by U. Högström (5), in case of a neutral atmosphere $\sigma_z(x, 0)$ may be written as:

$$\sigma_z(x, 0) = \frac{\sigma_w}{\bar{u}} \frac{1}{a_0} [2(e^{-a_0 x} + a_0 x - 1)]^{\frac{1}{2}} \qquad (17)$$

with

$$\sigma_w = (\overline{w'^2})^{\frac{1}{2}}$$

$$\frac{Ak\bar{u}}{\sigma_w} = k \frac{\bar{u}}{\bar{u}_*} \quad \text{where } A = 1.33 \qquad (16)$$

$$a_0 = \frac{\sigma_w}{\bar{u}.l_a \dfrac{K_M}{K_H}} \quad \text{and } l_a = k(z + z_0 + d)$$

where K_H and K_M are the eddy diffusivities for heat and momentum respectively.

For the Mol site, in neutral conditions, one has found:

$$\frac{\sigma_w}{\bar{u}} = 0.13$$

and $a_0 = 5.42 \times 10^{-3}$ with $K_M/K_H = 1$

Table 12

Downwind distance x	$\sigma_z(x, 0)$ Computed by (17)	Tests
100 m	12 m	14 m
1 000 m	71 m	73 m
10 000 m	247 m	370 m

The results of the comparison of $\sigma_z(x, |S|) \simeq 0)$ computed by (17) and directly determined by the observation of the wind vector fluctuations are shown in Table 12.

The agreement is excellent, at at least for short downwind distances.

The relative disagreement at $x = 10\,000$ m may be explained by the intervention of small frequency eddies which leads to a greater diffusion when the sampling time interval is 1 hour and also by the fact that those tests where σ_z was not proportional to $\sqrt{x}$ have been eliminated (see (1) pp. 79 to 81).

7.4. Tracer releases

7.4.1. *Mol experiments*

It has been thought essential to check the results obtained on the site at Mol through the observation of the fluctuating wind vector by comparing them to those resulting from tracer release experiments.

An aerosol generator has been installed on the meteorological mast at 69 m near the vectorial anemometer. It was especially designed to emit in the atmosphere in a regular and continuous manner 5 to 6 kg of fluorescein acid powder very finely divided (dimensions of the grains less than 4 μm) during about 50 minutes.

During each tracer release experiment, 50 to 80 collectors were placed along several arcs distant of 100 to 15 000 m from the source and centred on the presumed plume axis.

A quantitative analysis of the tracer collected on the filters was made using fluorimetric techniques. Thus the dilution factor $\chi\bar{u}/Q$ (m^{-2}) could be determined for each point of the observation network.

Fifteen experiments were completed in diverse types of meteorological conditions covering five of the six main atmospheric equilibrium categories E_1 to E_6. All aspects of these experiments are fully described in (1), chapter VI.

Results of the comparison: Table 13 gives the results of the evaluation of $\sigma_y(x)$ at different downwind distances from the source for experimental releases performed during E_1 to E_5 conditions.

The $\sigma_y(x)$ resulting from the measurements of the tracer concentrations near the ground were obtained by graphical estimation of the central angle of the arc limited at both ends by the points where one-tenth of the maximum concentration had been measured.

Table 14 gives the minimum values or the range of minimum values of the ratios of the computed dilution factors to the measured ones.

As can be seen from the examination of Tables 13 and 14:

1. The $\sigma_y(x)$ measured in the field are neither significantly nor systematically different from the computed ones.

2. The computed dilution factors are greater than the measured ones by a factor varying generally from 1.5 to 3 whatever may have been the weather conditions.

The fact must be emphasized that if σ_y and σ_z figures resulting from the use of the atmospheric stability categories are used in computations instead of the figures arising directly from the statistical treatment of the actual wind vector fluctuations, the conclusions above remain true as long as the mean direction of the wind has not significantly changed during the course of the experiment.

Another important remark is that all the causes of errors affecting tracer release technique–loss of powder in the aerosol generator, sedimentation, capture by the soil, impact on tree leaves and especially on pine-needles and decrease of fluorescence due to sunlight action–converge towards the determination of too small dilution factors.

7.4.2. *Tihange experiments*

Another tracer releases campaign (17), performed in E_3, E_4 and E_5 conditions only, has been carried out at the Tihange site situated in the river Meuse valley. A comparison between theoretical and practical data has given results very similar to those obtained at Mol despite the fact that the hilly Tihange site is very different from the practically flat S.C.K./C.E.N. site and that the source of the releases

Table 13

No.	Distance from source (m)	Significant change in mean wind direction	σ_y(m) from tracer release	σ_y(m) from wind vector fluctuations	Atmospheric stability category
F_3	500	yes	77	65	E_3
	1 700		170	192	
F_4	450	no	91	81	E_4
F_6	700	no	150	110	E_4
F_7	550	yes	190	220	E_5
F_8	200	no	41	55	E_5
F_{11}	2 000	no	105	95	E_2
	4 000		100	145	
F_{12}	3 300	yes	310	320	E_1
F_{13}	700	no	85	93	E_3
F_{14}	450	yes	96	100	E_5
F_{15}	2 500	no	142	120	E_2
F_{16}	2 100	no	68	95	E_1
	7 000		284	280	

was at a height of 150 m above the bottom of the valley (i.e. 70 to 90 m above the nearest hill tops).

7.5. Comparison with results of tracer release compaign at BNL

The extensive BNL tracer releases compaign, the results of which are given in (16), fig. 4.4, is particularly interesting to take as a comparison because the field rugosity, the duration of the sampling and the form given to the data were about the same as or could be made similar to the presentation at Mol. Ground concentrations due to releases at a height of 110 m are presented as $\chi\bar{u}/Q = f(x)$ for three types of anemonetric traces.

Table 15 gives the basic data regarding the BNL experiments as well as the corresponding atmospheric stability categories as determined in (1), chap. VI § 6.2.

The results are compared in Fig. 5 which shows that:

(a) the downwind distances $x_{\max}$ where the maximum dilution factors are almost the same at BNL and at Mol. As this distance depends on σ_z only, it appears that the Mol dispersions in the vertical plane are representative of the real behaviour of the atmosphere at least for categories E_6, E_4 and E_2 between 200 and 3 000 m from the source;

Table 14

Atmospheric stability category	Minimum value of ratio $\left(\frac{\chi\bar{u}}{Q}\right)_c \Big/ \left(\frac{\chi\bar{u}}{Q}\right)_m$	Distance from source where the minimum ratio was computed (m)
E_1	1.7	8 000
E_2	1.9–3.0	5 600
E_3	1.3–2.5	1 500
E_4	3.6	8 000
E_5	1.5–3.0	15 000

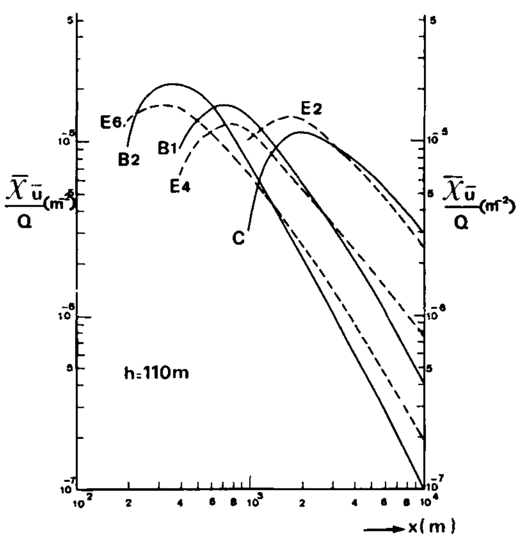

Fig. 5. Comparison between B.N.L. and C.E.N. results.

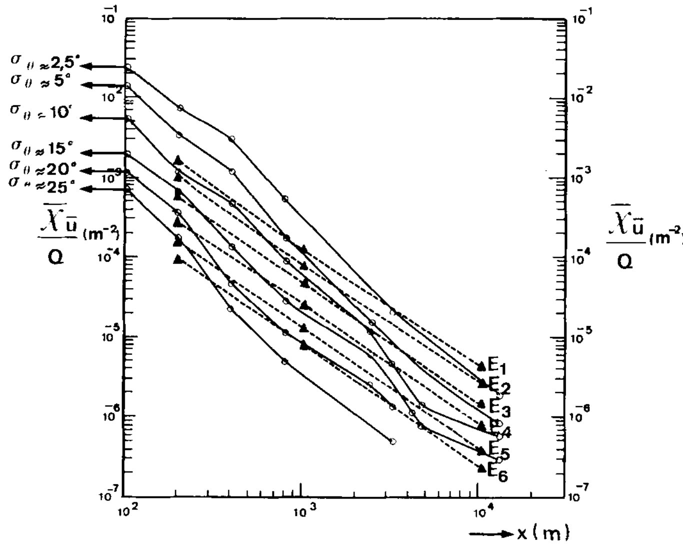

Fig. 6. Comparison between 200 tests made in the USA and the C.E.N. results.

(*b*) maximum concentrations obtained at Mol using the quick estimations of σ_y and σ_z are a little smaller (factor 1.3) for categories E_6 and E_4 and a little greater (factor 1.2) for category E_2 than the corresponding ones at BNL;

(*c*) concentrations at a great downwind distances (10 000 m) obtained at Mol are a little greater (factor 1.7) for categories E_6 and E_4 and a little smaller (factor 1.2) than those found at BNL. Due account being taken of experimental errors arising from the use of tracer release techniques, agreement between BNL and S.C.K./C.E.N. results is doubtless.

7.6. Comparison with 200 tracer releases from a ground source made in USA

The results of these 200 tracer releases are given in (15) as a function of the angular dispersion σ_θ.

Fig. 6 shows a comparison between these results and those of Mol. It may be seen immediately that the Mol σ_θ's are greater than the others especially when the atmosphere is stable. As mentioned before, this is due to the fact that the Mol. σ_θ's are evaluated at a height of 69 m; in stable conditions, the obstacles disseminated on the site generate great frequency eddies, the effect of which is more important at 69 m than near the ground.

At great downwind distances (10 000 m) the action of these eddies is strongly reduced and it is actually at these distances that the comparison becomes most interesting.

In fact, the agreement of the two sets of results is then remarkable. In particular, the range of variation of the dilution factors are the same (factor 20 between the data corresponding to very stable and very unstable weather conditions). This latter result has also been

Table 15

Type of anemometric traces	σ_θ(°)	$\bar{u}$ at $h = 107$ m (m.s^{-1})	Corresponding atmospheric equilibrium category
B_2	20	3	E_6 ($\sigma_\theta = 21°$)
B_1	13	7	E_4 ($\sigma_\theta = 14°$)
C	7	13	E_2 ($\sigma_\theta = 6.3°$)

confirmed by a tracer release campaign performed on the site of the nuclear power plant of the Ardennes (SENA) at Chooz. It is not so for F. Pasquill's results which show a much greater difference (several orders of magnitude) at large downwind distances due to the marked increase of Pasquill's σ_z's with x in very unstable conditions.

7.7. Conclusion

From the comparisons hereabove and their discussion, it seems reasonable to accept the Mol results proposed here for further application to the determination of diffusion characteristics of elevated continuous point sources emitting in most weather conditions encountered.

REFERENCES

1. Bultynck, H. & Malet, L. M., 1969. Diffusion turbulente des effluents émis dans l'atmosphère par une source élevée à émission continue en relation avec la stabilité de l'air. S.C.K./C.E.N., BLG 434, tome I (texte) p. 107 + annexes; tome II (figures).
2. Bultynck, H., Malet, L. M., Sharma, L. N. & van der Parren, J. 1970. Atmospheric dilution factors and calculation of doses in the environment of S.C.K./C.E.N. Mol for short and long duration stack discharges. S.C.K./C.E.N., BLG 446, tome I (text) p. 81; tome II (figures).
3. Wandel, C. F. & Kofoed-Hansen, O. R., 1962. On the Eulerian-Langrangian transform in the statistical theory of turbulence. *J. Geophys. Res. 67*, 3089.
4. Monin, A. S. & Obukhov, A. M., 1959. Smoke propagation in the surface layer of the atmosphere Intern. Symp. on Atmospheric diffusion and Air Pollution. *Adv Geophys 6*, 331–343.
5. Högström, U. 1964. An experimental study on atmospheric diffusion. *Tellus 16*, 2.
6. Pasquill, F., 1962. *Atmospheric diffusion.* D. van Nostrand Co. Ltd., London.
7. Lettau, J. F. & Davidson, B. 1957. *Exploring the atmosphere first mile*: Vol. I, Instrumentation and data evaluation; Vol. II, Site description and data tabulation. Pergamon Press, New York.
8. Schotsmans, L. 1968. Least squares solutions of m simultaneous non linear equations in *n* unknowns Newton Raphson iteration (RA-58). Internal note on Programming no. 47 C.E.N. Mol.
9. Healy, J. W. 1957. Calculations of environmental consequences of reactor accidents. HW-54128.
10. Pasquill, F. 1961. The estimation of the dispersion of windborne material. *Met. Mag. 90*, 33–49.
11. Hilsmeier, W. F. & Gifford, F. A. 1962. Graphs for estimating atmospheric dispersion. ORO-545.
12. Raynor, G. S. & Smith, M. E. 1964. A diffusion deposition tracer system. B.N.L. 859.
13. Smith, M. E. 1956. The variation of effluent concentrations from an elevated point source. *AMA Arch. Ind. Hlth. 14*, 56–58.
14. Stewart, N. G., Gale, H. J. & Crooks, R. N. 1954. The atmospheric diffusion of gases discharged from the chimney of the Harwell pile (BEPO). AERE HP/R 1452.
15. Slade, D. H. (Editor). 1968. Meteorology and atomic energy. A.E.C.–T.I.D.–24190.
16. Pasquill, F. 1962. Recent broad-band spectral measurements of turbulence in the lower atmosphere. *J. Geophys. Res. 67*, 3025.
17. Bultynck, H. & Osipenco, A. 1969. Résultats d'une campagne de rejets tracés réalisée sur le site nucléaire de Tihange (août–septembre–octobre 1969). S.C.K./C.E.N., Document interne.

ОЦЕНКА ВЕЛИЧИН ДИСПЕРСИИ В АТМОСФЕРЕ ДЛЯ ПРИМЕСЕЙ, ИСПУСКАЕМЫХ ПРИПОДНЯТЫМ НЕПРЕРЫВНЫМ ТОЧЕЧНЫМ ИСТОЧНИКОМ

Путем использования измерений с помощью трехкомпонентного анемометра флуктуаций вектора ветра на высоте 69 *м* были вычислены стандартные отклонения σ_y и σ_z для поперечных и вертикальных распределений примесей, испускаемых приподнятым непрерывным точечным источником. Было произведено почти 300 часовых испытаний, покрывающих большинство погодных условий, встречающихся на станции Мол. Определялись также величины параметра устойчивости S, вычисляемого как отношение часовых средних вертикального градиента потенциальной температуры между 8 и 114 *м* к квадрату среднечасовой скорости ветра на высоте 69 *м*. Зависимость функций $\sigma_{y,z} = f(S)$ имеет вид гипербол как для $S > 0$, так и для $S < 0$, что применимо для среднечасовых скоростей ветра вплоть до 11,5 *м*/сек. Для простоты и получения быстрых оценок величин σ_y и σ_z для текущих практических целей было определено семь категорий атмосферной устойчивости с соответствующими медианными значениями σ_y и σ_z при разных подветренных

расстояниях x. Когда $\bar{u} < 11{,}5$ *м*/сек, категории от E_1 до E_6 различаются с помощью параметра λ, определяемого как $\lambda = \lg 10^6 |S|$; категория E_7 относится к случаю сильных ветров. Полученные данные показывают, что для подветренных расстояний x до 50 *км* стандартные отклонения σ_y и σ_z зависят от x по степенному закону. Результаты расчетов хорошо согласуются с данными наблюдений на станции Мол и с данными наблюдений других авторов.